Hindawi Publishing Corporation
International Journal of Polymer Science
Volume 2012, Article ID 391325, 14 pages
doi:10.1155/2012/391325

Research Article

A Theoretical Study of the Insertion of Atoms and Ions into Titanosilsequioxane (Ti-POSS) in Comparison with POSS

Yosuke Komagata, Takaaki Iimura, Nobuhiro Shima, and Takako Kudo

Department of Chemistry and Chemical Biology, Graduate School of Engineering, Gunma University, 1-5-1 Tenjin-cho, Kiryu 376-8515, Japan

Correspondence should be addressed to Takako Kudo, tkudo@gunma-u.ac.jp

Received 9 June 2012; Revised 26 August 2012; Accepted 26 August 2012

Academic Editor: Kensuke Naka

The insertion reaction of various guest species, such as rare gases (He, Ne, and Ar), cations of group 1 (Li^+, Na^+, and K^+), and anions of group 17 (F^- and Cl^-) elements, into the Ti analogues of POSS (polyhedral oligomeric silsesquioxanes), Ti-POSS, $[HTiO_{1.5}]_n$ (n = 8 and 10), has been investigated by ab initio molecular orbital and density functional methods. For each case, the properties of the exohedral and endohedral complexes and transition-state structure connecting them on the potential energy surface and energetics are discussed in comparison with the case of POSS. Furthermore, in order to understand the origin of the stability of these structures, the binding energy (ΔE_{comp}) and the energy barrier of the encapsulation are analyzed by an energy decomposition method. As a result, some similarities and differences between Ti-POSS and POSS were explored.

1. Introduction

Polyhedral oligomeric silsesquioxanes (POSS), $[RSiO_{1.5}]_n$ (n = 4, 6, 8, 10, 12, ...), referred to as T_n, have been the focus of considerable experimental and theoretical interest because of their wide variety of practical uses for many years [1–4]. Among a huge number of investigations for these diverse polyhedral compounds, the approach to make use of their cavity for various purposes, such as a container of atomic or molecular species [5–19], medical supplies [20, 21], molecular sieves, or a reaction filed for H_2 formation [22], is one of the extremely attractive research areas of the POSS chemistry. In addition to many interesting experimental observations, theoretical studies have been making considerable contributions in this area. For example, there are systematic and comprehensive studies for the encapsulation of various atomic or ionic species into T_8 and T_{10} by Hossain et al. [9, 13, 15, 16]. Furthermore, incorporation of molecular species such as H_2, N_2, and O_2 inside T_n (n = 6–12) that also been investigated by our group [5, 18, 19]. These studies must give useful information for the future design of the molecular sieve or better drug delivery.

On the other hand, metal-substituted POSS (metallasilsesquioxanes) where the skeletal silicon atoms of POSS are all or partially replaced with various metals such as group 4 (Ti, Zr, and Hf) [23–29] or other heavier group 14 (Ge Sn) [29] elements are also fascinating research targets. The titanosilsequioxanes especially (Ti-T_n) have extensively been studied both by experimental and theoretical chemists because of their potential as useful materials such as promising catalysts. For the experimental works, the titanium-substituted T_8 with the $TiSi_7O_{12}$ core [24, 26] and even the Si/Ti-alternated T_8 with the $Ti_4Si_4O_{12}$ core [23, 25] have already been synthesized and their stability or catalytic activity investigated years ago. On the other hand, not for Ti-POSS but some theoretical studies on the structures and catalytic reactions of the model compounds of titanosilicate or titanium-containing zeolites are available [30, 31]. In the past several years, therefore, we have studied the structures and catalytic ability of the titanium analogues of POSS, $[HTiO_{1.5}]_n$ and $H_8Ti_pSi_{8-p}O_{12}$ [27]. Incidentally, the experimental result [23] for the structure of the Si/Ti-alternated T_8 is in good agreement with our calculational result [27]. Our next target is their various intramolecular

Table 1: Some geometrical parameters (Å and degrees), the averaged net atomic charge, [a]energy level of HOMO and LUMO, and the HOMO-LUMO energy gap (hartree)[c] of Ti-T_8 and Si-T_8 at the B3LYP/6-311+G(d) level.

A	A-O	A-H	<AOA	<OAO	C^b-A	C^a-O
Si	1.644	1.460	148.4	109.2	2.744	2.690
Ti	1.811	1.697	149.1	109.1	3.023	2.951
A	q_A[a]	q_o[a]	HOMO[c]	LUMO[c]	$\Delta E^c_{(H\text{-}L)}$	
Si	2.131 (0.767)	−1.268 (−0.474)	−0.319 [−0.483]	−0.007 [0.052]	0.312 [0.535]	
Ti	1.313 (0.202)	−0.787 (−0.110)	−0.328 [−0.464]	−0.139 [0.019]	0.189 [0.483]	

[a]NBO and Mulliken (in parentheses) net atomic charges on A (Si and Ti) and O atoms.
[b]C is the center of the cage.
[c]The HF/6-311+G(d) values are in square brackets.

reactions. Therefore, in the present study, as a continuation of our theoretical approach for Ti-POSS and to deepen our understanding for POSS, the result of the investigation for the encapsulation of various atoms and ions into Ti-T_8($[HTiO_{1.5}]_8$) is shown and discussed in comparison with the case of the Si analogue, T_8($[HSiO_{1.5}]_8$).

2. Computational Methods

Geometry optimizations were performed for all of the molecules investigated here at the Hartree-Fock (HF) and a hybrid type of the HF and DFT theories, B3LYP [32] levels of theory. For the basis set, 6-311+G(d) [33–35] was finally chosen after the investigation of several kinds of basis sets. We have investigated the effect of six kinds of basis sets (6-31G(d), 6-311G(d), 6-31+G(d), 6-31G(d,p), 6-31+G(d,p), and 6-311+G(d)) for the geometries of exohedral and endohedral complexes between X (He and F^-) and Ti-T_8 at the HF and B3LYP levels of theory. As a result, a set of p functions on hydrogen atoms is found to have small effect so it was not considered in this study. All optimized geometries were characterized as minima or transition states by normal frequency mode analyses. In addition, single point energy calculations on the optimized geometries were carried out at the second-order perturbation (MP2) [36] level of theory for a part of the system involving F^- to obtain more reliable energetics. Finally, the relative energies of the stationary points were corrected by considering the zero point energy (described as "+ZPC").

Furthermore, in order to explore the origin of the stability of the stationary points on the potential energy surface of the encapsulation reactions in detail, we carried out a kind of energy decomposition for the binding energy (ΔE_{comp}) between the guest species and the host Ti-T_n cage. The ΔE_{comp} is the energy accompanying the formation of complexes (exohedral and endohedral complexes, and the transition-state structures connecting them), and it is decomposed into two kinds of energy—(a) the deformation energy (ΔE_{def}) of the host cage caused by the complexation, and (b) the interaction energy (ΔE_{int}) between the guest species and the deformedhost cage:

$$\Delta E_{comp} = \Delta E_{def} + \Delta E_{int}. \quad (1)$$

The former always brings about the destabilization of the system, but even the latter is possible to contribute the destabilization (repulsion) as well as the stabilization. The "minus" value means stabilization, while "plus" does destabilization of the system relative to the referred one for the binding energy (ΔE_{comp}) and both energy components, ΔE_{def} and ΔE_{int}.

The ΔE_{def} is obtained as the energy difference between the deformed cage ($E_{deformed\ cage}$) and the optimized (empty) one ($E_{pure\ cage}$):

$$\Delta E_{def} = E_{deformed\ cage} - E_{pure\ cage}. \quad (2)$$

On the other hand, the ΔE_{int} is defined as the energy difference between the complexes (E_{comp}) and the sum of two energy components as shown as follows:

$$\Delta E_{int} = E_{comp} - \left(E_{deformed\ cage} + E_{guest\ species}\right). \quad (3)$$

As a result, the ΔE_{comp} can be described as another formula as expected:

$$\Delta E_{comp} = E_{comp} - \left(E_{pure\ cage} + E_{guest\ species}\right). \quad (4)$$

All calculations were performed with the Gaussian 03 [37] and GAMESS [38, 39] electronic structure codes.

3. Results and Discussion

3.1. Ti-T_8 versus Si-T_8. Before discussing the encapsulation reaction, it may be worth to compare some properties of the host molecule, Ti-T_8, $(HTiO_{1.5})_8$, with those of the Si analogue, T_8, $(HSiO_{1.5})_8$. Both molecules have highly symmetric O_h structure [27]. The geometric parameters, the averaged NBO [40] and the Mulliken net atomic charge of the skeletal atoms, and the energy levels of the frontier orbitals (the Kohn-Sham orbitals in the DFT results) of both molecules are shown in Table 1. As the table shows, all distances in Ti analogue are longer than those in T_8, suggesting Ti–T_8 has the larger cavity compared to that of the Si analogue. It is convenient for the encapsulation of guest species as well as the extremely floppy titanoxane (Ti–O–Ti) bonds in the framework suggested by our previous study [27]. The two kinds of the bond angles, however, are very similar in both molecules.

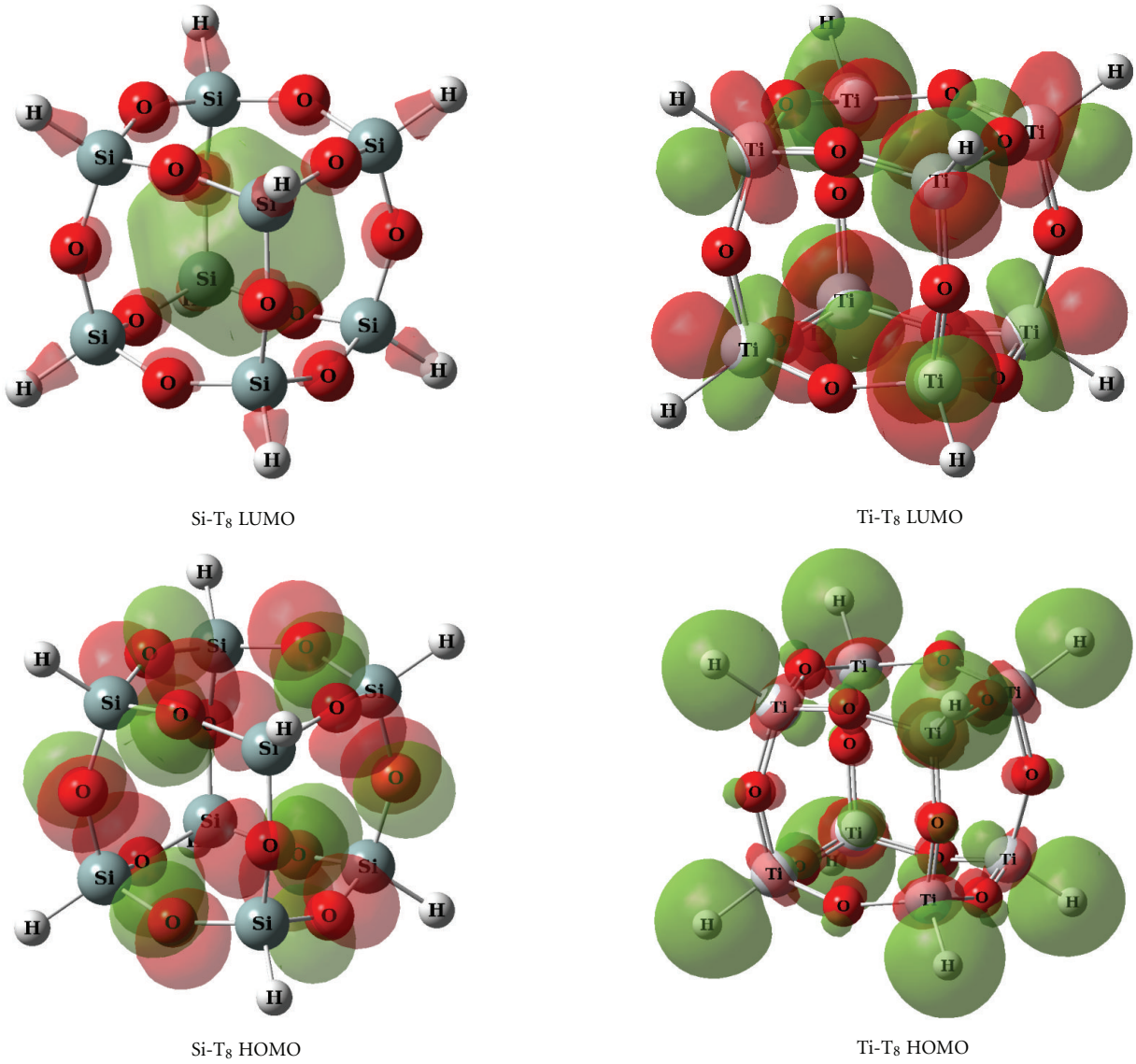

Figure 1: The HOMO and LUMO of T_8 and Ti-T_8 at the B3LYP/6-311+G(d) level.

In addition, the averaged net atomic charges in the table suggest that the Ti–O bond is less polarized compared to the Si–O, which is in agreement with our previous results for the siloxane and titanoxane compounds ($H(OH)_2XOX(OH)_2H$; X = Si and Ti) [29]. In the Si/Ti-mixed POSS, however, Ti atom is found to have larger positive charge than that of Si atoms [27]. As the present basis set involves the diffuse functions, absolute values of the Mulliken charge seem to be remarkably underestimated compared to those of the NBO charge.

On the other hand, the B3LYP level significantly underestimates the HOMO-LUMO gap compared to the corresponding value obtained at the HF level, as expected. According to the HF results, the HOMO is higher and LUMO is lower in Ti-T_8 than in T_8, which makes the HOMO-LUMO energy gap of the T-T_8 slightly smaller compared to that of T_8. Nevertheless, the figures of the orbitals, especially for HOMO, are very similar in the HF and B3LYP levels. As seen from Figure 1, the d orbitals on Ti atoms seem to play an important role for both frontier orbitals in Ti-T_8 while the contribution of the p orbitals on oxygen atoms seems to be large in T_8.

3.2. Insertion of Rare Gas Elements (He, Ne, and Ar). In Scheme 1 displayed is the schematic process of the insertion of some rare gas elements and cations into Ti-T_8. As seen in the scheme, the guest species and Ti-T_8 form exohedral complex (X(Ti-T_8)) where the rare gas elements are above the center of a D_4 ($(HTiO)_4$) face of the cage first. Then the species inserts into the host cage via the transition-state structure with keeping the same C_{4v} symmetry as the first complex. The resultant endohedral complex (X@(Ti-T_8)) has the guest species in the center of the cage so the symmetry is as high as D_{4h} (O_h).

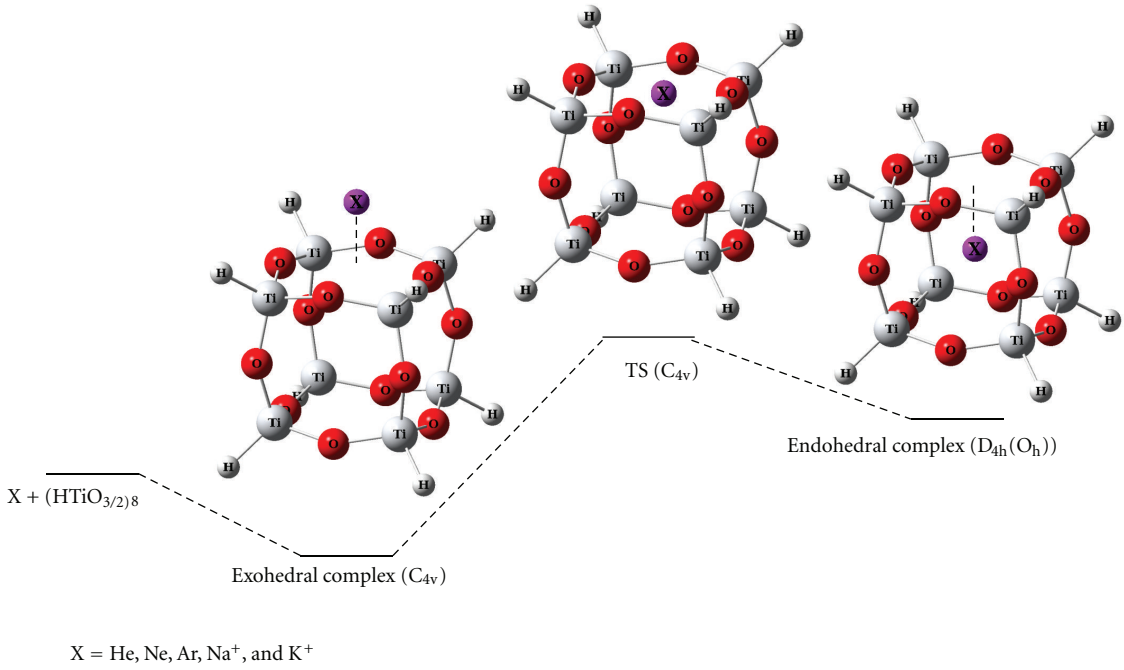

Scheme 1

The B3LYP/6-311+G(d) geometries of these structures are depicted in Tables 2 and 3. For the exohedral complexes, as Table 2 shows, the attached species X is far from the cage (>3 Å). Also, for the endohedral complexes, the geometry of the host cage does not largely change by the inclusion of guest species except for the heaviest rare gas element in this study, Ar atom. On the other hand, for the transition-state structures (see Table 3), the geometry of the D_4 face where the insertion takes place is remarkably expanded and the extent becomes large as the atomic radius of the guest element becomes large in the order He < Ne < Ar as expected. The other faces are not much affected as seen in the H_2 insertion into POSS [18].

The energetics of the insertion reaction in Table 4 show that the energy barrier increases as the atomic radius of the guest element increases as expected from the geometrical change mentioned above. Apparently, the inclusion complex is less stable than the exohedral complex but that may be possible to exist because of the large release energy in all cases.

On the other hand, the binding energies (ΔE_{comp}) together with the result of energy decomposition are summarized in Table 5. For the rare gas elements, ΔE_{comp} and the two energy components (ΔE_{def} and ΔE_{int}) of the exohedral complex are very small. Furthermore, the absolute values of the deformation energy (ΔE_{def}) of the endohedral complex and the transition structure are much smaller than those of the interaction energy (ΔE_{int}). These results suggest that the encapsulation of the rare gas elements has just a small effect for the cage of Ti-T_8 and the origin of the binding energy is mainly the repulsion with the cage and not the deformation of the cage.

The reaction mechanism and the structures of the stationary points are similar to those of the Si analogue by Park et al. [9].

3.3. Insertion of Cations of Alkali Metal Elements (Li^+, Na^+, and K^+). The insertion reaction discussed next is that of the cations of three alkali metal (group 1) elements. Among these, the reaction of the Na^+ and K^+ resembles that of the rare gas elements and the structures of the stationary points are also similar. For the exohedral complexes, the distance between the cations and the cage is smaller than that of the rare gases as shown in Table 2. The same is true in the r(X-O), while the opposite (longer) is seen in the r(X-Ti), for the endohedral complexes. This may be explained from the electrostatic interaction between the plus charge of the guest cations and skeletal $Ti^{\delta+}$ and $O^{\delta-}$ atoms of the host. Such interaction especially in the endohedral complex of Na cation is considered to be significant as the symmetry of the structure of Na^+@Ti-T_8 is reduced from D_{4h} to C_{2v}. This is in sharp contrast to the fact that the Si analogue keeps the highest symmetry in the endohedral complex, Na^+@T_8 [9].

In contrast, the both complexes of Li^+ are quite different with other cases as shown in Figure 2. There is another exohedral complex (exo-2) in addition to the normal C_{4v} structure (exo-1). As the figure shows, Li^+ is attached on one of the skeletal oxygen atoms in "exo-2" while the cation interacts with all oxygen atoms of the D_4 face in "exo-1" and the former is 0.6 kcal/mol less stable than the latter. Furthermore, two types of the endohedral complex ("endo-1" and "endo-2") were located as in the case of the Si analogue [9]. The "endo-1" has the stretched cubic structure with the D_{4h} symmetry, while in "endo-2" the cage is remarkably deformed

Table 2: Some geometrical parameters (Å and degrees) of X(Ti-T_8) and X@(Ti-T_8); X = He, Ne, Ar, Na^+, K^+, Cl^- at the B3LYP/6-311+G(d) level.

X	X(Ti-T_8) (exohedral complex)				X@(Ti-T_8) (endohedral complex)					
	sym	r(X-S[a])	r(X-Ti)	r(X-O)	sym	r(X-S[a])	r(X-Ti)	r(X-O)	<TiOTi	<OTiO
Pure					D_{4h}	1.746	3.023	2.950	149.1	109.1
He	C_{4v}	4.217	4.885	4.396	D_{4h}	1.748	3.028	2.950	149.4	108.9
Ne	C_{4v}	3.504	4.284	3.782	D_{4h}	1.750	3.031	2.954	149.3	109.0
Ar	C_{4v}	5.292	5.838	5.365	D_{4h}	1.757	3.043	2.975	148.8	109.3
Na^+	C_{4v}	2.119	3.247	2.545	C_{2v}	1.716	3.069	2.595	154.9	103.1
K^+	C_{4v}	2.769	3.698	3.028	D_{4h}	1.790	3.101	2.892	157.2	104.7
Cl^-					D_{4h}	1.707	2.959	3.053	139.1	113.7

[a]The center of a D_4 face.

Table 3: Some geometrical parameters (Å and degrees) of the D_4 face where the insertion takes place in the transition structure connecting X(Ti-T8) and X@(Ti-T8); X = He, Ne, Ar, Na^+, K^+, Cl^- at the B3LYP/6-311+G(d) level.

X	sym	r(X-Ti)	r(X-O)	r(Ti-O)	<TiOTi	<OTiO
Pure	D_{4h}	2.468	2.114	1.811	149.1	109.1
He	C_{4v}	2.503	2.160	1.833	148.4	112.7
Ne	C_{4v}	2.510	2.267	1.860	143.5	119.0
Ar	C_{4v}	2.553	2.431	1.924	138.7	126.5
Na^+	C_{4v}	2.629	2.107	1.889	159.6	103.5
K^+	C_{4v}	2.676	2.299	1.951	150.7	112.7
Cl^-	C_{4v}	2.440	2.507	1.906	129.5	136.7

Table 4: The B3LYP/6-311+G(d)+ZPC relative energy (kcal/mol) of the exohedral (X(Ti-T8)) and endohedral (X@(Ti-T8)) complexes (X = He, Ne, Ar, Li^+, Na^+, K^+, and Cl^-) and the transition state (TS) connecting them and the release energy (ΔE) of X from the endohedral complex.

X	X(Ti-T_8)	TS	X@(Ti-T_8)	Release ΔE
He	0.0	31.2	7.6	23.6
Ne	0.0	58.3	11.6	46.7
Ar	0.0	145.2	46.0	99.2
Li^+	0.0	27.8	25.8	2.0
Na^+	0.0	60.7	31.7	29.0
K^+	0.0	150.9	53.6	97.3
Cl^-	0.0	83.5	7.7	75.8

compared to "endo-1." The large deformation of the cage in both structures is brought about by the strong interaction between Li^+ and skeletal oxygens as indicated by the short Li–O distances of 2.181 and 2.081 Å in the planar or tetrahedral Li^+O_4 moiety of "endo-1" and "endo-2," respectively. As a result, the symmetry of "endo-2" is reduced to D_{2d}, and this is found to be more stable than "endo-1" by 2.2 kcal/mol at the B3LYP/6-311+G(d) +ZPC level. These are the same trend in the $Li^+@T_8$ [9].

Figure 3 shows the potential energy surface of the insertion of Li^+ into Ti-T_8. The exo-2 and endo-1 are not involved in the figure. It is noteworthy that Li^+ seems to keep some interaction with several specific oxygens during the insertion process as the transition-state structure is not symmetric with respect to the center.

The energetics of the insertion reaction of these cations can be compared with those of rare gas elements in Table 4. The energy changes with regard to atomic number in both groups resemble each other. As the atom becomes heavy in each group, the energy barrier becomes high and the endohedral complex becomes less stable. However, the stability of the endohedral complex relative to the exohedral complex is smaller in the cations compared to the rare gas elements. For the case of Li^+, especially the release energy is too small (2.0 kcal/mol) for Li^+@Ti-T_8 to exist stably. As a result, for the encapsulation of Li^+ in Ti-T_8, only the exohedral complex is predicted to be existable. On the other hand, the endohedral complex of the other cations is kinetically existable but the energy barrier is too high for the exohedral complex to isomerize to the endohedral complex at least in the room temperature.

As Table 5 shows, the deformation energy (ΔE_{def}) of the exohedral complex of the cations is much larger than that of the rare gas elements as expected from the significant

Table 5: Energy decomposition of the binding energy (ΔE_{comp}) (kcal/mol) of the complexes of various guest species and Ti-T8 and the transition state connecting the complexes at the B3LYP/6-311+G(d) level.

	X	sym	ΔE_{def}	ΔE_{int}	ΔE_{comp}	ΔE_{comp} + ZPC
Exo	He	C_{4v}	0.0	−0.2	−0.2	−0.1
	Ne	C_{4v}	0.0	−0.3	−0.3	−0.2
	Ar	C_{4v}	0.0	0.0	0.0	0.0
	Li^+	C_{4v}/C_1	17.4/11.8	−56.9/−50.6	−39.5/−38.8	−38.1/−37.5
	Na^+	C_{4v}	11.7	−33.9	−22.2	−21.6
	K^+	C_{4v}	7.9	−19.9	−12.0	−11.8
	Cl^-	Cs	35.9	−93.6	−57.7	−57.4
Endo	He	D_{4h}	0.1	6.6	6.7	7.5
	Ne	D_{4h}	0.1	10.6	10.7	11.4
	Ar	D_{4h}	1.4	43.7	45.1	46.0
	Li^+	D_{2d}/D_{4h}	31.9/27.7	−45.9/−39.0	−14.0/−11.3	−12.3/−10.1
	Na^+	C_{2v}	16.3	−6.6	9.7	10.1
	K^+	D_{4h}	15.4	25.7	41.1	41.8
	Cl^-	D_{4h}	17.3	−67.5	−50.2	−49.7
TS	He	C_{4v}	2.0	27.3	29.3	31.1
	Ne	C_{4v}	10.2	47.0	57.2	58.1
	Ar	C_{4v}	39.4	106.0	145.4	145.2
	Li^+	C_s	28.3	−40.0	−11.7	−10.3
	Na^+	C_{4v}	22.2	15.6	37.8	39.1
	K^+	C_{4v}	45.6	93.7	139.3	139.1
	F^-	C_1/C_1	50.6/52.8	−136.9/−131.6	−86.3/−78.8	−85.7/−77.9
	Cl^-	C_{4v}	59.0	−32.2	26.8	26.1

geometrical changes mentioned above. The host cage is considerably destabilized as suggested by the large value of ΔE_{def}, but the stabilization by ΔE_{int} overwhelms the disadvantage so the complex becomes more stable than the isolated cation and cage eventually in all cases. The large plus values of ΔE_{def} (destabilization) and large minus values of ΔE_{int} (stabilization) in the cation complexes compared to those of the rare gases may be explained from the electrostatic interaction between the plus charge of the cations and the skeletal elements. For all stationary points of the cations, as ionic radius becomes small, ΔE_{def} becomes large (destabilized) and ΔE_{int} becomes small (largely minus, stabilized) except for ΔE_{def} of the transition-state structure of K^+. Here, it may be interesting to compare the ΔE_{int} of isoelectronic pairs, He/Li^+, Ne/Na^+, and Ar/K^+. The NBO analyses [40] show the plus charge of the free cations (formally 1) is significantly reduced by the complexation, such as Li^+ (exo-1/exo-2 : 0.777/0.912, end-1/endo-2 : 0.509/0.495), Na^+ (exo: 0.883, endo: 0.484), and K^+ (exo: 0.943, endo: 0.558), suggesting the considerable electrostatic interaction with the host cage and this brings about the large stability of the complexes indicated by the largely minus ΔE_{comp}.

For the endohedral complex of the cations, however, the destabilization caused by the significant geometrical changes mentioned above is more serious compared to the exohedral complexes, as indicated by the larger value of ΔE_{def}. The strong interaction between the cations and skeletal atoms may be the main reason for the large ΔE_{def} as suggested from the geometrical parameters in Table 2. As a result, ΔE_{comp} is still minus for the Li^+@Ti-T_8 while K^+@Ti-T_8 gives remarkably plus value so severe steric repulsion between the guest with large ionic radius and host may be expected in the case of K^+. The value of Na^+@Ti-T_8 is the intermediate between the cases of Li^+ and K^+. Incidentally, ΔE_{comp} of the transition-state structure for the Li^+ case is minus, −11.7 (−10.3 with ZPC) kcal/mol, too. This minus value is caused by the largely minus ΔE_{int} as shown in Table 5. This stabilization may be explained from the unique structure (Figures 2 and 3) mentioned above and makes the TS of the insertion of Li^+ lower compared to that of the other cations and the endohedral complex kinetically unstable.

3.4. Insertion of Anions of Halogen Elements (F^- and Cl^-). Next guests are the minus ions of halogen (group 7). The structures of the complexes and reaction paths of the halogen anions investigated here (especially F^-) are significantly different with those of the rare gas or cationic elements in the preceding sections. Incidentally, there are many comprehensive studies for the encapsulation of F^- into POSS, and it is well known that the endohedral complex F^-@T_8 has been observed experimentally [7, 8, 12].

First, the properties of the complexes between the halogen anions and Ti cage are explained in detail. For F^-, as Figure 4 shows, various kinds of exohedral ((a)–(d)) and endohedral (e) complexes were located but we could not find the exohedral structure with the higher C_{4v} symmetry like the rare gas or cationic species. F^- tends to interact strongly with small number (1 or 2) of skeletal Ti atoms. Among

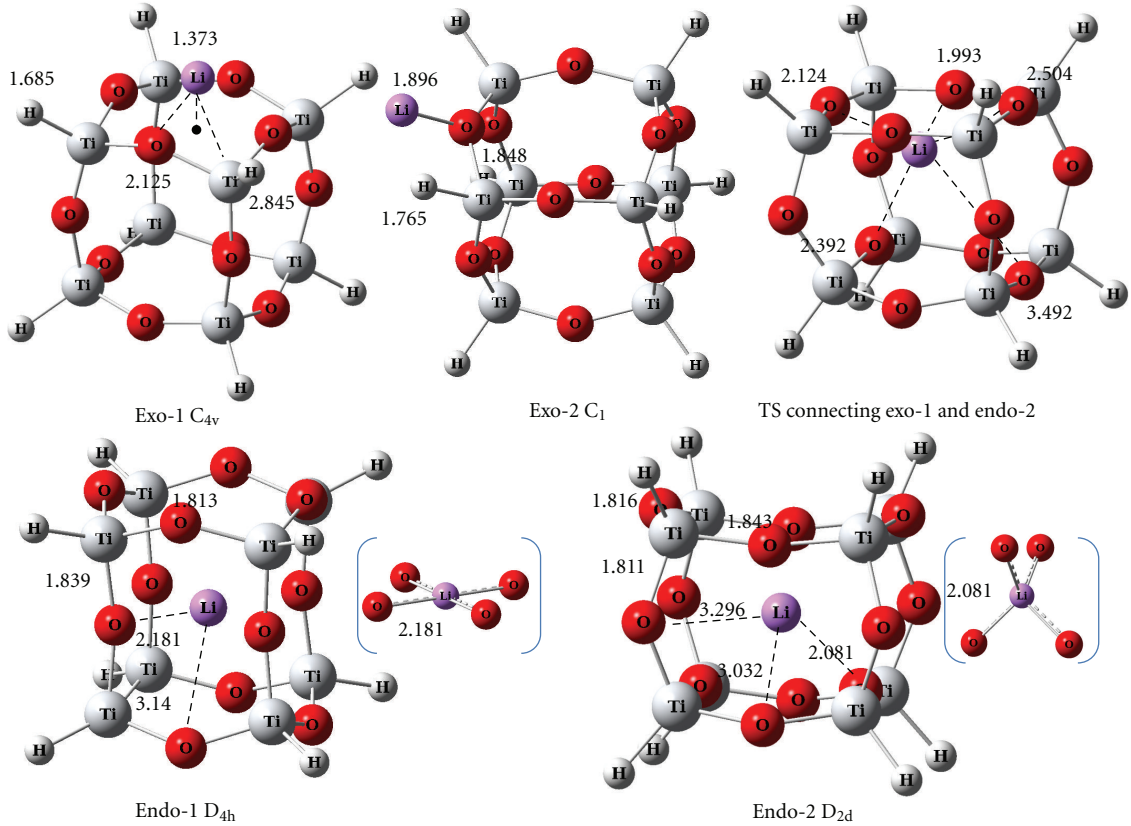

FIGURE 2: The B3LYP/6-311+G(d) optimized geometries of the exohedral and endohedral complexes and the transition state connecting "Exo-1" and "Endo-2" of Li^+ and Ti-T_8 in angstroms.

these, (a) and (b) have the partial triangular bipyramidal structure so we call each of them as "axial" and "equatorial" complex, respectively (see Scheme 2). The similar exohedral complexes are observed in the Si analogue too, though the "equatorial" conformation is not an equilibrium structure [9]. F^- interacts with one Ti atom in (a) and (b) while it does with more than two Ti atoms in the others in Figure 4. Apparently in the diagonally bridged structures, "diagonal-bridge" (d), the Ti-T_8 cage is considerably deformed as suggesting with the largest ΔE_{def}, so it is remarkably less stable than other isomers as seen in Table 6.

On the other hand, the structure of the endohedral complex "endo" (e) is quite interesting since F^- is notthe center of the cage but close to a specific skeletal Ti atom, which is completely different with the initial expectation. As a result, this complex also seems to have the partial triangular bipyramidal structure with F^- at the axial position in a corner of the cage. This is also different with the fact that the F^- is encapsulated in the center of the silicon analogue, T_8 [9]. Nevertheless, Tossell has found that in the larger POSS such as T_{10} and T_{12} with the double-decker structure F^- is bound at the Si atom in a corner of the cage so the present result resembles that [12].

The distance between F^- and the Ti in (e) is 2.321 Å so it is rather longer than 1.814 Å in (a). As apparent from Table 6, the smallest deformation energy among the isomers suggests that this structure does not bring about such a severe energetic damage of the cage seen in the other structures. That is the reason why the endohedral complex (e) is most stable in spite of the smallest interaction energy among the five isomers. The relative stability was found to increase (−3.2 to −7.6 kcal/mol) at the more reliable MP2 level. In order to confirm whether the small space of T_8 triggers such a unique structure, we have investigated the case of larger Ti-T_{10}. However, as Figure S1 (in Supporting Information available online at doi:10.1155/2012/391325) shows, the similar endohedral (endo) complex was also located, and the F-Ti distance is ca. 0.1 Å shorter than that in "endo" (e) of Ti-T_8. Interestingly, in contrast, it is found that Ti-T_6 with a smaller titanoxane cage (a prismatic shape) has a F^- in the center of the cage like in the case of F^-@T_8 at the same B3LYP/6-311+G(d) level (see Figure S2). This means the cavity of Ti-T_8 is large enough for a F^- moves rather freely compared with that of Ti-T_6. Therefore, the limited space of Ti-T_8 is found not to be the reason for the strange behavior of F^- in the endohedral complex but the strong electrostatic interaction between F^- and Ti atom of Ti-T_n (n = 8 and 10) may be the plausible explanation. Furthermore, in consideration of the Tossell results for F^-@T_n (n = 10 and 12) [12], F^- seems to prefer to interact with a specific Ti or Si rather than with plural skeletal atoms at the same time if there is enough space to allow that in the cage.

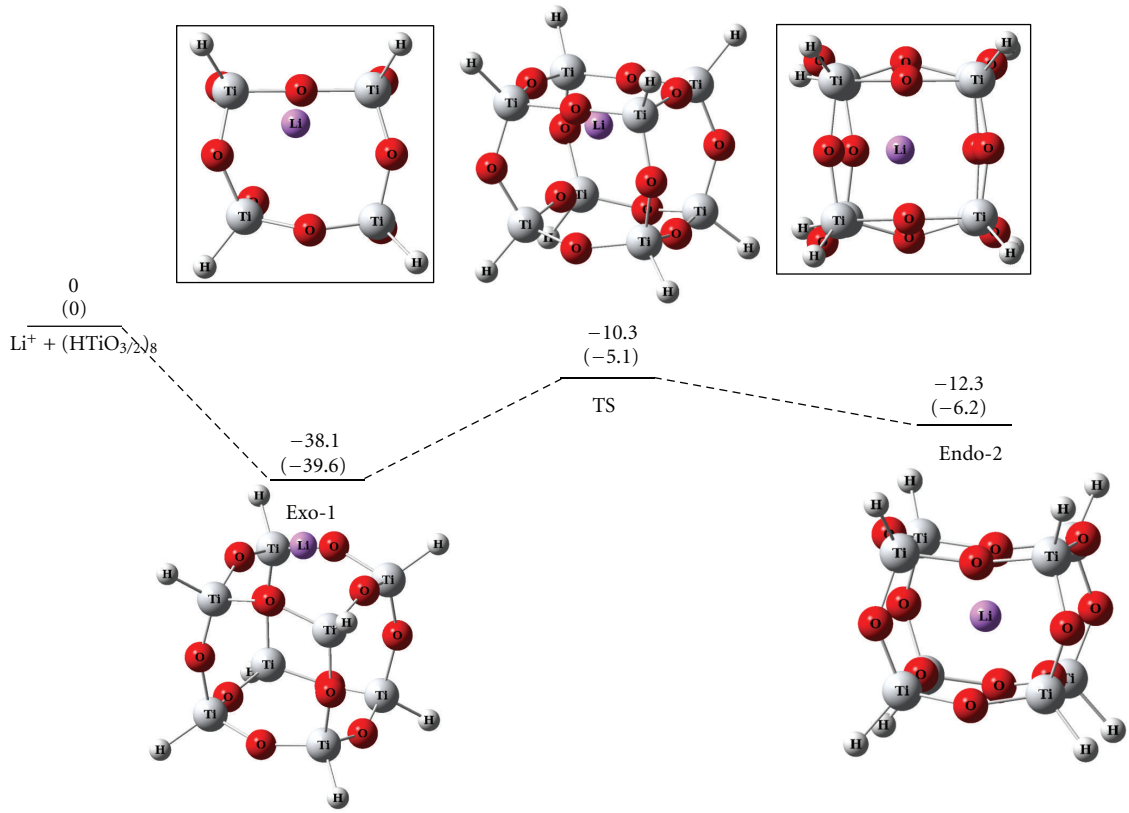

Figure 3: The potential energy surface (kcal/mol) of the insertion reaction of Li^+ into Ti-T_8 with the structures of the exohedral complex (Exo-1), the transition state (TS), and endohedral complex (Endo-2) at the B3LYP/6-311+G(d)+ZPC and HF/6-311+G(d)+ZPC (in parentheses) levels. For the transition state, the side view is in the left quadrangle while the top view is in the right one.

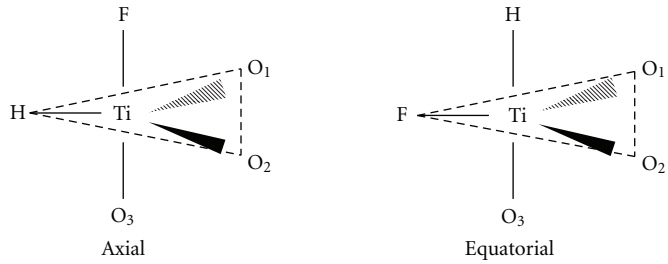

Scheme 2

On the other hand, the isomerization between "axial" and "equatorial" exohedral complexes of F^-(Ti-T_8) takes place via the transition structure also shown in Figure 4. The "equatorial" structure is less stable than "axial" by 3.6 (2.7 at the HF/6-311+G(d)+ZPC level) kcal/mol at the B3LYP/6-311+G(d)+ZPC level, while the extremely low energy barrier (0.3 kcal/mol at the HF level) needed for the isomerization to "axial" is further reduced to less than 0.1 kcal/mol at the B3LYP level. Therefore, for the exohedral complex of F^-(Ti-T_8), "axial" is the main structure but the interconversion of the two conformations is possible to take place very easily.

In contrast with the F^- case, the situation of the encapsulation of Cl^- into Ti-T_8 cage is quite simple. The "axial" is a unique exohedral complex and the endohedral complex has a Cl^- at the center of the cage with the D_{4h} symmetry like those of the rare gases and K^+ as shown in Figure 5. As seen from Table 4, the endohedral complex is less stable only by 7.7 kcal/mol than the exohedral complex. This is in sharp contrast with the fact that the endohedral complex is largely less stable than the exohedral complex in the isoelectronic Ar and K^+ as shown in Table 4. This is explained from the small ΔE_{def} (17.3 kcal/mol) and large absolute value of the ΔE_{int} (−67.5 kcal/mol) of the endohedral complex of Cl^-@Ti-T_8 (see Table 5). As a result, the endohedral complex is not so unstable compared to the other cases.

Incidentally, the deformation energy (ΔE_{def}) of the complexes of F^- and Ti-T_8 is larger than that of the complexes of Cl^- and Ti-T_8 probably because of the larger geometrical

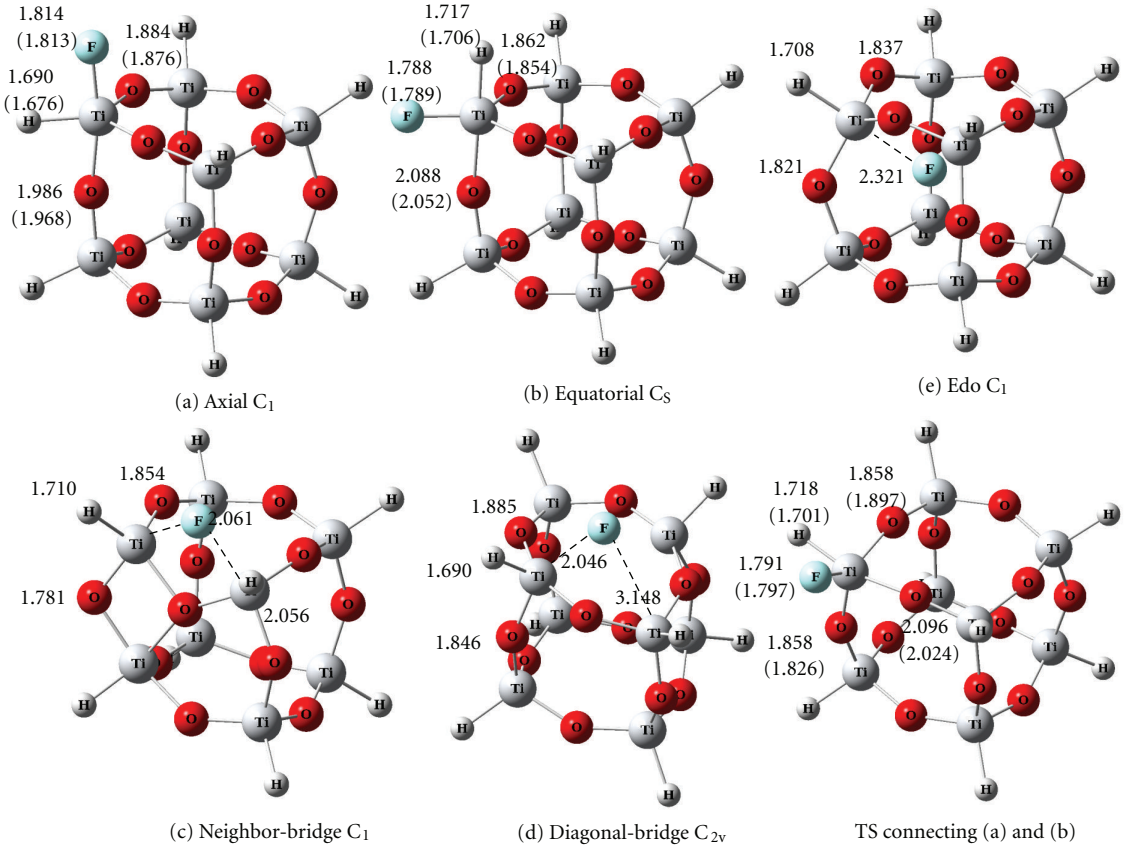

(a) Axial C_1 (b) Equatorial C_S (e) Edo C_1

(c) Neighbor-bridge C_1 (d) Diagonal-bridge C_{2v} TS connecting (a) and (b)

Figure 4: The B3LYP/6-311+G(d) and HF/6-311+G(d) (in parentheses) optimized geometries of exohedral and endohedral complexes of F^- and Ti-T_8 and the transition state for the "Axial" (a) "Equatorial" (b) isomerization in angstroms.

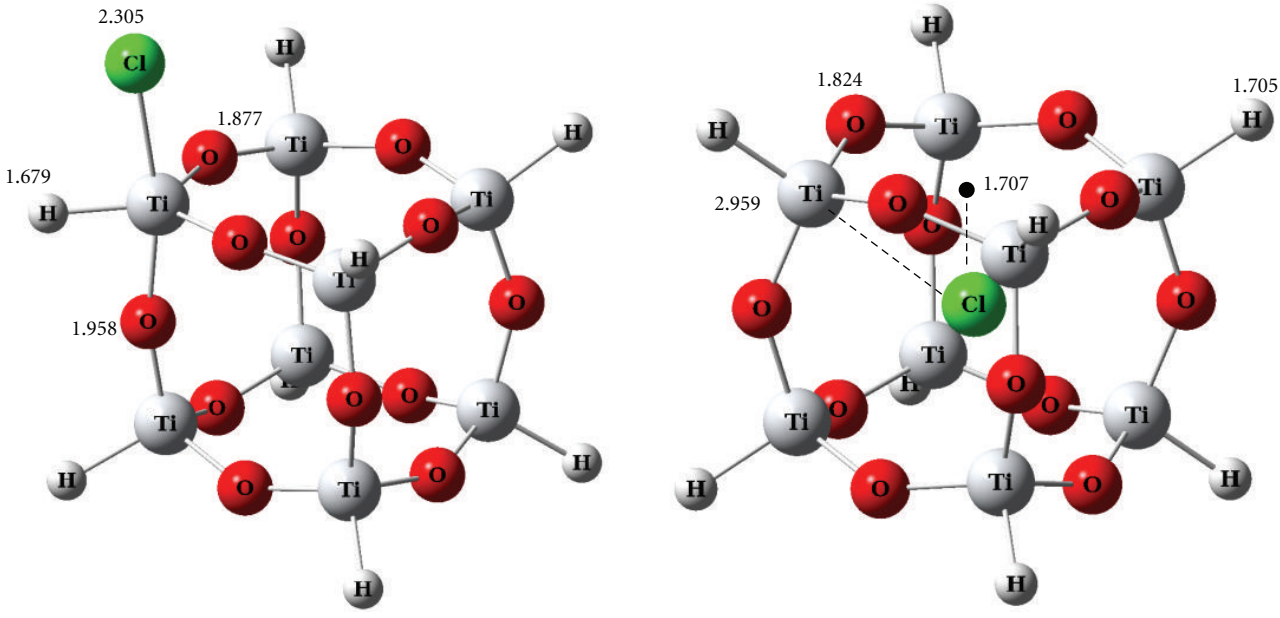

(a) Axial C_s (b) Endo D_{4h}

Figure 5: The B3LYP/6-311+G(d) optimized geometries of the exohedral (Axial) and endohedral (Endo) complexes of Cl^- and Ti-T_8 in angstroms.

Table 6: Energy decomposition of the binding energy (ΔE_{comp}) (kcal/mol) of the complexes of F^- and Ti-T_8 and the energies relative to "axial" (ΔE) in each system based on the B3LYP/6-311+G(d)+ZPC and MP2/6-311+G(d)//B3LYP/6-311+G(d)[a] energies.

	Isomer	Sym	ΔE_{def}	ΔE_{int}	ΔE_{comp}	ΔE_{comp} + ZPC	ΔE
F^-+Ti-T_8	(a) Axial	C_1	35.9	−135.1	−99.1	−98.4	0.0 [*0.0*]
	(b) Equatorial	Cs	55.6	−150.6	−95.0	−94.8	3.6
	(c) Neighbor bridge	C_1	56.3	−151.4	−95.1	−93.7	4.7
	(d) Diagonal bridge	C_{2v}	63.9	−149.5	−85.6	−84.7	13.7
	(e) Endo	C_1	23.2	−125.3	−102.1	−101.6	−3.2 [*−7.6*]

[a]The values in italics are in square brackets.

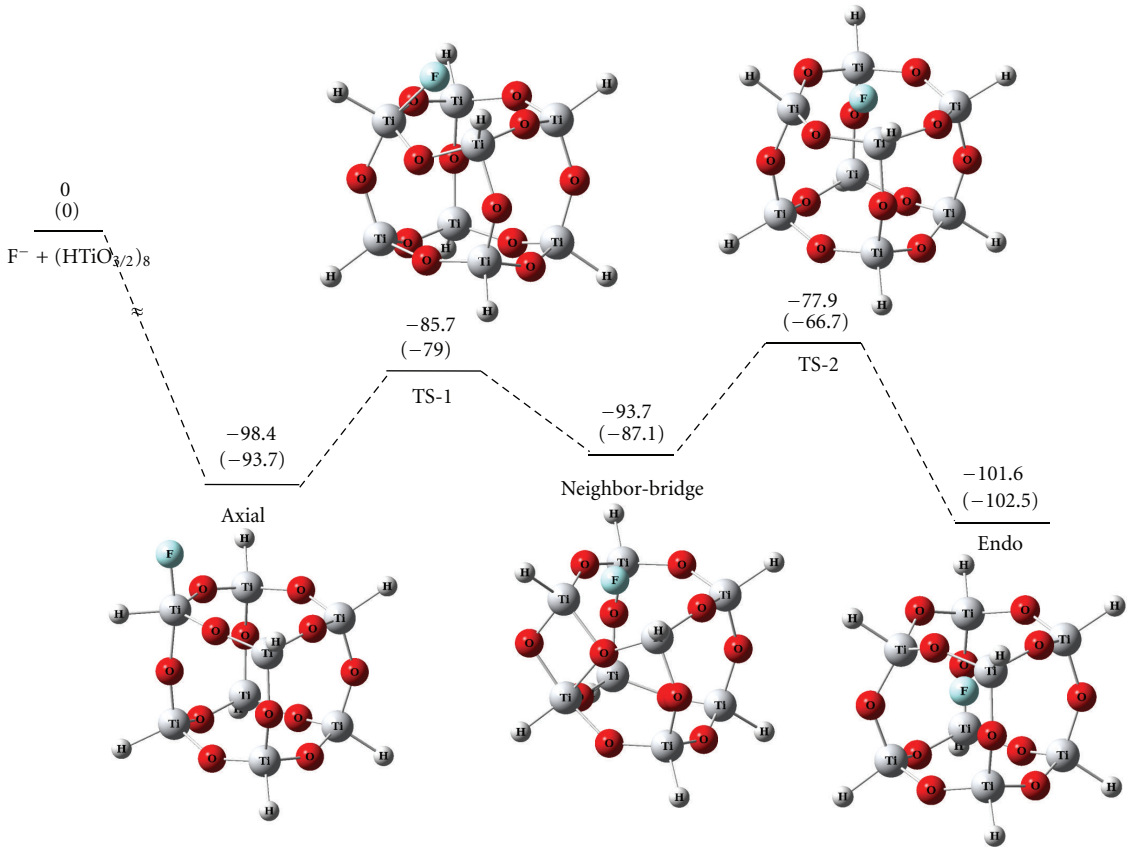

Figure 6: The potential energy surface (kcal/mol) of the insertion reaction of F^- into Ti-T_8 with the structures of some stationary points at the B3LYP/6-311+G(d)+ZPC and HF/6-311+G(d)+ZPC (in parentheses) levels.

changes. This is the same trend in the relation between Li^+ and the heavier cations (Na^+ and K^+). That is, as the element of the group is lighter (smaller), it is able to interact with specific skeletal atoms in the cage, which brings about the larger deformation of the host cage.

On the other hand, the NBO charge of Cl^- in the endohedral complex Cl^-@Ti-T_8 is −0.427 while that of F^- in F^-@Ti-T_8 is −0.688. This result suggests that the larger amount of minus charges is transferred from Cl^- to the cage compared to the case of F^- and the considerable electrostatic interaction between Cl^- and the cage because of the large ionic radius even at the center of the cage.

The last topic of this section is the reaction mechanisms of the encapsulation of the halogen anions into Ti-T_8. The potential energy surface of F^- and Cl^- is displayed in Figures 6 and 7, respectively. In both cases, the formation reaction of the exohedral complex (axial) is largely exothermic in energy. However, the following process is one-step reaction for Cl^- while two-step reaction for F^- because the "neighbor-bridge" structure exists between the exohedral and endohedral complexes for the latter as displayed in Figure 6. The "neighbor-bridge" complex has a diamond-shaped Ti_2O_2 part in the strained structure. From the complex to the second TS (TS-2), the F^- falls down into the cage with pushing out the oxygen of the flexible titanoxane (Ti–O–Ti) bond to outside of the cage. As a result, the rhombus Ti_2O_2 structure is broken down and the energy needed for the motion brings about the second energy barrier of

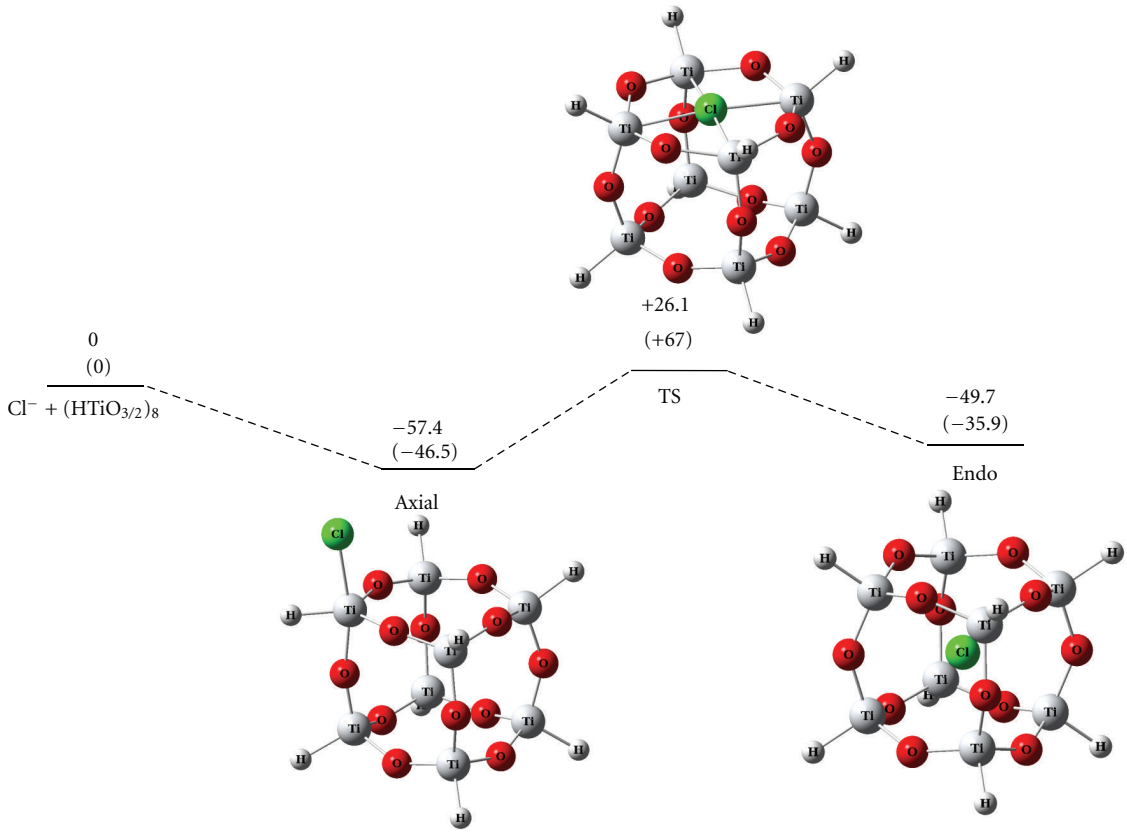

Figure 7: The potential energy surface (kcal/mol) of the insertion reaction of Cl^- into Ti-T_8 with the structures of the exohedral (Axial) and endohedral (Endo) complexes and the transition state (TS) connecting them at the B3LYP/6-311+G(d)+ZPC and HF/6-311+G(d)+ZPC (in parentheses) levels.

the reaction. All stationary points are lower than the reactants in energy. Therefore, the encapsulation of F^- into Ti-T_8 is predicted to take place rather easily. In fact, the absolute value of the ΔE_{comp} (−102.1 kcal/mol) of the endohedral complex of F^- and Ti-T_8 is largest among all species investigated in this study. In the silicon analogue, $F^-@T_8$ has already been observed experimentally so the Ti analogue may also be observed in near future.

For the encapsulation of Cl^-, the anion inserts from the center of the D_4 face as indicated from the TS structure in Figure 7. For the silicon analogue, $Cl^-@T_8$, the siloxane bond seems to be partially broken in the transition-state structure of the insertion and it could not keep the highly symmetric structure probably because of the smaller size of the cage [9]. As Figure 7 shows, the transition state "TS" for the insertion of Cl^- into Ti-T_8 is higher than the reactants in energy, which is different with the F^- case but rather resembles to the rare gas elements and Na^+ and K^+ except for the fact that the endohedral complex is lower than the reactants.

3.5. Comparison with POSS. Finally, we compare the present results for the insertion reactions with those of the Si analogues (T_8) in order to clarify the characteristics of the Ti compounds. As already mentioned frequently, the same reaction of T_8 has been investigated comprehensively by Park et al. [9] and the results are referred to in the preceding sections. Therefore, we just mention here the comparison of energetics of the reaction of Ti-T_8 and T_8 at the same level of theory in Table 7.

The trend of the binding energy (ΔE_{comp}), relative energies of the complexes, and the transition structures on the potential energy surface are similar for both compounds. The ΔE_{comp} of the exohedral complex of all elements except for Ar is minus, suggesting that these complexes are easily formed energetically. In addition, as the element becomes heavy, the relative stability of the transition state and endohedral complex becomes small probably because of their steric repulsion. Furthermore, the steric repulsion may explain that their relative energies are always larger in T_8 than in Ti-T_8 as the size of the cage of the former is smaller. Only one exception is the endohedral complex of $F^-@T_8$. The remarkable stability may be the reason why the complex has been observed experimentally. Also, the endohedral complex (endo) of $F^-@$Ti-T_8 is more stable than the exohedral (axial) complex though the relative stability is smaller than the Si analogue.

Furthermore, we should note that the considerably small release energy of the endohedral complex between Li^+ and Ti-T_8, $Li^+@$Ti-T_8. This is the same trend as the corresponding silicon complex. As already noted, therefore, the inclusion complex of Li^+ and Ti-T_8 may be hardly observed experimentally.

Table 7: The energetics (kcal/mol) of the encapsulation of X (X = He, Ne, Ar, Li^+, Na^+, K^+, F^-, and Cl^-) into A-T_8 (A = Si and Ti) at the B3LYP/6-311+G (d)+ZPC and MP2/6-311+G(d)[a] levels on the B3LYP/6-311+G(d) optimized geometries.

X	A-T_8 A	ΔE_{comp} of exo	Relative energy			Release energy
			Exo	TS	Endo	
He	Ti	−0.1	0.0	31.2	7.6	23.6
	Si	−0.1	0.0	54.3	13.2	41.1
Ne	Ti	−0.2	0.0	58.3	11.6	46.7
	Si	−0.1	0.0	109.5	24.1	85.4
Ar	Ti	0.0	0.0	145.2	46.0	99.2
	Si	0.0	0.0	252.9	95.9	157.0
Li^+	Ti	−38.1	0.0	27.8	25.8	2.0
	Si	−46.3	0.0	35.0	28.0	7.0
Na^+	Ti	−21.6	0.0	60.7	31.7	29.0
	Si	−29.3	0.0	107.2	40.3	66.9
K^+	Ti	−11.8	0.0	150.9	53.6	97.3
	Si	−17.7	0.0	237.1	85.8	151.3
F^-	Ti	−98.4	0.0 (0.0)	12.7/20.5	−3.2 (−7.6)	23.7
	Si	−58.6	0.0	65.9	−13.2	79.1
Cl^-	Ti	−57.4	0.0	83.5	7.7	75.8
	Si	−14.3	0.0	90.6	42.1	48.5

[a] The values are in parentheses.

4. Concluding Remarks

In the present work, the insertion reaction of various guest species such as rare gas, cations of the group 1, and anions of the group 17 elements, into the Ti analogue of T_8, Ti-T_8, has been investigated in comparison with the case of the Si analogue.

For rare gas elements, the mechanism of the insertion is the same as that of the Si analogue, T_8; (1) formation of the exohedral complex where the atom is above the center of a D_4 ($(HTiO)_4$) face, (2) interaction from the center of a D_4 in the transition-state structure, and (3) formation of the endohedral complex with the atom in the center of the cage. The interaction with the host is rather small for all cases, and the energy for the encapsulation (energy barrier for the isomerization of exohedral to endohedral complexes) becomes large as the element becomes heavy.

On the other hand, for the cations of the group 1 elements, the reaction mechanism between Li^+ and the heavier elements (Na^+ and K^+) is different. The latter group is rather similar to the rare gas elements in the geometries of the complexes and transition state, but Li^+ is found to interact with specific skeletal oxygen atoms and form two types of structures in both complexes as a result. Binding energy of all the complexes between Li^+ and Ti-T_8 is largely minus, suggesting that the complex of the cation and Ti-T_8 is energetically more stable than the corresponding complex between rare gas elements and Ti-T_8. Furthermore, Li^+ interacts with the skeletal oxygen strongly in the exohedral complexes and the transition state for the encapsulation, which seems to make important contribution for their stability. As a result, the final product of the reaction, an endohedral complex, Li^+@Ti-T_8, is found to be kinetically unstable so only the exohedral complex may be existable.

Finally, for the anionic species of the group 17 elements, the behavior of F^- is considerably unique. Several kinds of complexes are located for the reaction between F^- and Ti-T_8, while two types (exohedral and endohedral) of complexes are located for the case of Cl^-. It may be worth to note that especially the position of a F^- is not the center of the cage in the endohedral complex but it takes the quasitriangular bipyramidal conformation at a corner of the cage. This is in sharp contrast with the fact that F^- is in the center of the cage in the corresponding complex of the Si analogue, F^-@T_8. The same thing was also seen in the endohedral complex of F^-@Ti-T_{10}, while F^- was found to be the center of the cage in smaller Ti-T_6. Therefore, the larger room of the Ti-T_8 and Ti-T_{10} compared to the corresponding Si cages as well as the strong electrostatic interaction between F^- and Ti atom may allow the unique structure. Furthermore, this prediction can explain the observation in F^-@Si-T_{10} and F^-@Si-T_{12} where F^- is bound at the corner of the cage [11, 12].

In summary, for the present encapsulation reaction of Ti-T_8, we found quite a few similar properties with those of the silicon analogue, T_8, in spite of the considerable difference in the nature of the skeletal bond and size of the cage. This means the reaction is mainly affected by the size of the host cage and not the skeletal elements. However, for the reaction of Ti-POSS, the strong interaction between the ionic species and a part of the skeletal atoms is still expected to play an important role. As an extension of the present study, therefore, an investigation of the intra-molecular catalytic reaction inside Ti-POSS is now in progress.

The discussion for the cage effect in the F^-@Ti-T_n ($n = 8$ and 10) (Figures S1–S3 and Tables S1 and S2), see the supplementary material available online at doi: 10.1155/2012/391325.

Acknowledgment

This work was partly supported by the "Element Innovation" Project by Ministry of Education, Culture, Sports, Science and Technology in Japan.

References

[1] M. G. Voronkov and V. L. Lavrent'yev, " Polyhedral oligosilsesquioxanes and their homo derivatives," *Topics in Current Chemistry*, vol. 102, pp. 199–236, 1982.

[2] F. J. Feher, D. A. Newman, and J. F. Walzer, "Silsesquioxanes as models for silica surfaces," *Journal of the American Chemical Society*, vol. 111, no. 5, pp. 1741–1748, 1989.

[3] R. H. Baney, M. Itoh, A. Sakakibara, and T. Suzuki, "Silsesquioxanes," *Chemical Reviews*, vol. 95, no. 5, pp. 1409–1430, 1995.

[4] F. J. Feher and T. A. Budzichowski, "Silasesquioxanes as ligands in inorganic and organometallic chemistry," *Polyhedron*, vol. 14, no. 22, pp. 3239–3253, 1995.

[5] B. Tejerina and M. S. Gordon, "Insertion mechanism of N_2 and O_2 into T_n ($n = 8, 10, 12$)-silsesquioxane framework," *Journal of Physical Chemistry B*, vol. 106, no. 45, pp. 11764–11770, 2002.

[6] L. A. Villaescusa, P. Lightfoot, and R. E. Morris, "Synthesis and structure of fluoride-containing GeO_2 analogues of zeolite double four-ring building units," *Chemical Communications*, no. 19, pp. 2220–2221, 2002.

[7] A. R. Bassindale, M. Pourny, P. G. Taylor, M. B. Hursthouse, and M. E. Light, "Fluoride-Ion encapsulation within a silsesquioxane cage," *Angewandte Chemie*, vol. 42, no. 30, pp. 3488–3490, 2003.

[8] A. R. Bassindale, D. J. Parker, M. Pourny, P. G. Taylor, P. N. Horton, and M. B. Hursthouse, "Fluoride ion entrapment in octasilsesquioxane cages as models for ion entrapment in zeolites. Further examples, X-ray crystal structure studies, and investigations into how and why they may be formed," *Organometallics*, vol. 23, no. 19, pp. 4400–4405, 2004.

[9] S. S. Park, C. Xiao, F. Hagelberg, D. Hossain, C. U. Pittman Jr., and S. Saebo, "Endohedral and exohedral complexes of polyhedral double four-membered-ring (D4R) units with atomic and ionic impurities," *Journal of Physical Chemistry A*, vol. 108, no. 51, pp. 11260–11272, 2004.

[10] G. Satre, A. Pulido, and A. Corma, "Pentacoordinated germanium in AST zeolite synthesised in fluoride media. A ^{19}F NMR validated computational study ," *Chemical Communications*, vol. 2005, pp. 2357–2359, 2005.

[11] M. Pach, R. M. Macrae, and I. Carmichael, "Hydrogen and deuterium atoms in octasilsesquioxanes: experimental and computational studies," *Journal of the American Chemical Society*, vol. 128, no. 18, pp. 6111–6125, 2006.

[12] J. A. Tossell, "Calculation of ^{19}F and ^{29}Si NMR shifts and stabilities of F^- encapsulating silsesquioxanes," *The Journal of Physical Chemistry C*, vol. 111, pp. 3584–3590, 2007.

[13] D. Hossain, C. U. Pittman Jr., S. Saebo, and F. Hagelberg, "Structures, stabilities, and electronic properties of endo-And exohedral complexes of T10-polyhedral oligomeric silsesquioxane cages," *Journal of Physical Chemistry C*, vol. 111, no. 17, pp. 6199–6206, 2007.

[14] S. E. Anderson, D. J. Bodzin, T. S. Haddad et al., "Structural investigation of encapsulated fluoride in polyhedral oligomeric silsesquioxane cages using ion mobility mass spectrometry and molecular mechanics," *Chemistry of Materials*, vol. 20, no. 13, pp. 4299–4309, 2008.

[15] D. Hossain, C. U. Pittman Jr., F. Hagelberg, and S. Saebo, "Endohedral and exohedral complexes of T8-polyhedral oligomeric silsesquioxane (POSS) with transition metal atoms and ions," *Journal of Physical Chemistry C*, vol. 112, no. 41, pp. 16070–16077, 2008.

[16] D. Hossain, S. R. Gwaltney, C. U. Pittman, and S. Saebo, "Insertion of transition metal atoms and ions into the nanoscale dodecahedral silsesquioxane (T12-POSS) cage: structures, stabilities and electronic properties," *Chemical Physics Letters*, vol. 467, no. 4–6, pp. 348–353, 2009.

[17] A. R. Geoge and C. R. A. Catlow, "An investigation into the effects of ion incorporation on the electronic structure of silicate fragments via ab initio computational techniques," *Chemical Physics Letters*, vol. 247, no. 4–6, pp. 408–417, 1995.

[18] T. Kudo, M. Akasaka, and M. S. Gordon, "Ab initio molecular orbital study of the insertion of H_2 into POSS compounds," *Theoretical Chemistry Accounts*, vol. 120, no. 1–3, pp. 155–166, 2008.

[19] T. Kudo, "Ab initio molecular orbital study of the insertion of H2 into poss compounds 2: the substituent effect and larger cages," *Journal of Physical Chemistry A*, vol. 113, no. 44, pp. 12311–12321, 2009.

[20] C. McCusker, J. B. Carroll, and V. M. Rotello, "Cationic polyhedral oligomeric silsesquioxane (POSS) units as carriers for drug delivery processes," *Chemical Communications*, vol. 8, pp. 996–998, 2005.

[21] H. Yuan, K. Luo, Y. Lai et al., "A novel poly(l-glutamic acid) dendrimer based drug delivery system with both pH-sensitive and targeting functions," *Molecular Pharmaceutics*, vol. 7, no. 4, pp. 953–962, 2010.

[22] T. Kudo, T. Taketsugu, and M. S. Gordon, "Ab initio molecular dynamics study of H_2 formation inside POSS compounds," *The Journal of Physical Chemistry A*, vol. 115, pp. 2679–2791, 2011.

[23] A. Voigt, R. Murugavel, V. Chandrasekhar et al., "Facile and rational route for high-yield synthesis of titanasiloxanes from aminosilanetriols," *Organometallics*, vol. 15, no. 6, pp. 1610–1613, 1996.

[24] M. Crocker, R. H. M. Herold, A. G. Orpen, and M. T. A. Overgaag, "Synthesis and characterisation of titanium silasesquioxane complexes: soluble models for the active site in titanium silicate epoxidation catalysts," *Journal of the Chemical Society, Dalton Transactions*, no. 21, pp. 3791–3804, 1999.

[25] R. Murugavel, P. Davis, and V. S. Shete, "Reactivity studies, structural characterization, and thermolysis of cubic titanosiloxanes: precursors to titanosilicate materials which catalyze olefin epoxidation," *Inorganic Chemistry*, vol. 42, no. 15, pp. 4696–4706, 2003.

[26] K. Wada, N. Itayama, N. Watanabe, M. Bundo, T. Kondo, and T. A. Mitsudo, "Synthesis and catalytic activity of group 4 metallocene containing silsesquioxanes bearing functionalized silyl groups," *Organometallics*, vol. 23, no. 24, pp. 5824–5832, 2004.

[27] T. Kudo and M. S. Gordon, "Structures and stabilities of titanium silsesquioxanes," *The Journal of Physical Chemistry A*, vol. 105, no. 50, pp. 11276–11294, 2001.

[28] T. Kudo and M. S. Gordon, "Ab initio study of the catalytic reactivity of titanosilsesquioxanes and titanosiloxanes," *Journal of Physical Chemistry A*, vol. 107, no. 41, pp. 8756–8762, 2003.

[29] T. Kudo, M. Akasaka, and M. S. Gordon, "Ab initio molecular orbital study on the Ge^-, Sn^-, Zr^- and Si/Ge-mixed silsesquioxanes," *The Journal of Physical Chemistry A*, vol. 112, no. 21, pp. 4836–4843, 2008.

[30] A. J. M. de Man and J. Sauer, "Coordination, structure, and vibrational spectra of titanium in silicates and zeolites in comparison with related molecules. An ab initio study," *The Journal of Physical Chemistry*, vol. 100, no. 12, pp. 5025–5034, 1996.

[31] P. E. Sinclair and C. R. A. Catlow, "Quantum chemical study of the mechanism of partial oxidation reactivity in titanosilicate catalysts: active site formation, oxygen transfer, and catalyst deactivation," *The Journal of Physical Chemistry B*, vol. 103, no. 7, pp. 1084–1095, 1999.

[32] A. D. Becke, "Density-functional thermochemistry. III. The role of exact exchange," *The Journal of Chemical Physics*, vol. 98, no. 7, pp. 5648–5652, 1993.

[33] M. M. Francl, W. J. Pietro, W. J. Hehre et al., "Self-consistent molecular orbital methods. XXIII. A polarization-type basis set for second-row elements," *The Journal of Chemical Physics*, vol. 77, no. 7, pp. 3654–3665, 1982.

[34] T. Clark, J. Chandrasekhar, G. W. Spitznagel, and P. V. R. Schleyer, " Efficient diffuse function-augmented basis sets for anion calculations. III. The 3-21+G basis set for first-row elements, Li-F," *Journal of Computational Chemistry*, vol. 4, pp. 294–301, 1983.

[35] M. J. Frish, J. A. Pople, and J. S. Binkley, "Self-consistent molecular orbital methods 25. Supplementary functions for Gaussian basis sets," *The Journal of Chemical Physics*, vol. 80, pp. 3265–3269, 1984.

[36] J. A. Pople, R. Seeger, and R. Krishnann, "A semi-empirical MO theory for ionization potentials and electron affinities," *International Journal of Quantum Chemistry*, vol. 11, pp. 149–163, 1977.

[37] M. J. Frisch, G. W. Trucks, H. B. Schlegel et al., *Gaussian 03, Revision C. 02*, Gaussian, Wallingford, Conn, USA, 2004.

[38] M. W. Schmidt, K. K. Baldridge, J. A. Boatz et al., "General atomic and molecular electronic structure system," *Journal of Computational Chemistryvol*, vol. 14, pp. 1347–1363, 1993.

[39] M. S. Gordon and M. W. Schmidt, "Advances in electronic structure theory: GAMESS a decade later," in *Theory and Applications of Computational Chemistry*, C. E. Dykstra, G. Frenking, K. S. Kim, and G. E. Scuseria, Eds., chapter 41, Elsevier, San Diego, Calif, USA, 2005.

[40] J. P. Foster and F. Weinhold, "Natural hybrid orbitals," *Journal of the American Chemical Society*, vol. 102, no. 24, pp. 7211–7218, 1980.